Acta Metallurgica Sinica (English Letters) (2020) 33:1226–1234
https://doi.org/10.1007/s40195-020-01036-w

Microstructure and Mechanical Properties of Mg–3Al–Zn Magnesium Alloy Sheet by Hot Shear Spinning

Fenghua Wang[1,4] · Peng Su[2] · Linxin Qin[1] · Shuai Dong[1] · Yunliang Li[3] · Jie Dong[1]

Received: 29 September 2019 / Revised: 9 January 2020 / Published online: 28 April 2020
© The Chinese Society for Metals (CSM) and Springer-Verlag GmbH Germany, part of Springer Nature 2020

Abstract
Hot shear spinning experiments with Mg–3.0Al–1.0Zn–0.5Mn (AZ31B, wt%) magnesium alloy sheets were conducted at various temperatures, spindle speeds and feed ratios to investigate the effects of these processing parameters on the microstructure, crystallographic texture and mechanical properties. The AZ31B sheet displayed good shear formability at temperatures from 473 to 673 K, spindle speeds from 300 to 600 rev/min and feed ratios from 0.1 to 0.5 mm/rev. During the dynamic recrystallization process, the grain size and texture were affected by the deformation temperature of the hot shear spinning process. Each of the spun sheets presented a strong basal texture, and the *c*-axis of most of the grains was parallel to the normal direction. The optimal hot shear spinning parameters were determined to be a temperature of 473 K, a spindle speed of 300 rev/min and a feed ratio of 0.1 mm/rev. The yield strength, ultimate tensile strength and elongation in the rolled direction reached 221 MPa, 288 MPa and 14.1%, and those in the transverse direction reached 205 MPa, 280 MPa and 12.4%, respectively. The improved strength and decreased mechanical anisotropy resulted from the fine grain size and strong basal texture.

Keywords AZ31B magnesium alloy · Shear spinning · Texture · Grain refinement

1 Introduction

Shear spinning is an effective method of manufacturing thin-walled rotational components. During the plastic deformation process, a sheet clamped with a tailstock rotates with a mandrel, and a roller pushes the sheet to the mandrel surface in one pass. Shear spinning is commonly used to produce structural components in the automotive and aerospace industries due to its low forming forces and high precision [1, 2]. Magnesium (Mg) alloys have recently attracted significant interest for structural applications due to their low density and high specific strength [3, 4]. Therefore, it is highly desirable to achieve high strength and toughness in Mg alloy production via shear spinning.

Mg alloys are known to exhibit poor formability at room temperature due to an insufficient number of independent slipping systems [5–9]. To improve its formability, hot forming processes such as rolling and extrusion have been successfully developed. Non-basal slip can be easily activated when the deformation temperature exceeds 473 K. Dynamic recrystallization is also an efficient way to release work hardening [9–14]. Many recent studies have examined hot flow forming and shear spinning in Mg alloys. Cao et al. [15] examined the effects of temperature, feed rate, spindle speed and thickness reduction on the microstructure and mechanical properties of AZ80 alloy after hot flow forming. They showed that the optimal tensile properties were obtained at a temperature of 693 K, a spindle speed of 400 rev/min, a feed ratio of 0.1 mm/rev and a thickness reduction of 45%. Zhang et al. [16] analysed the effects of a reduction in thickness on grain refinement and texture evolution during the hot

Available online at http://link.springer.com/journal/40195.

✉ Jie Dong
jiedong@sjtu.edu.cn

[1] National Engineering Research Center of Light Alloy Net Forming and State Key Laboratory of Metal Matrix Composites, Shanghai Jiao Tong University, Shanghai 200240, China

[2] Sinopec Northwest Oilfield Company, Urumqi 830011, China

[3] School of Mechanical Engineering, Shanghai Jiao Tong University, Shanghai 200240, China

[4] Shanghai Light Alloy Net Forming National Engineering Research Center Co. Ltd, Shanghai 201615, China

flow forming of AZ31B alloy. Their results indicated that the microstructure was refined and became uniform when the reduction in thickness reached 45% and the *c*-axis of most grains was approximately parallel to the radial direction. Li et al. [17] used hot shear spinning experiments to analyse the effects of process parameters on the formability of AZ31 alloy and obtained the following optimal parameters: a diameter-to-thickness ratio of sheet blank of 18, a spinning temperature of 573 K and a swivel angle of 35°. The deformation behaviour and microstructure of $AlMg_6Mn$ alloy subjected to shear spinning with thickness reductions of 30%, 50% and 68% were studied with mechanical tests, optical and scanning electron microscopy and energy-dispersive X-ray spectroscopy [18]. The results showed that as its thickness decreased, the grain structure gradually became more refined, elongated in the axial direction and stretched in the circumferential direction. However, few researchers have focused on the microstructure and mechanical properties of rolled AZ31B sheet after hot shear spinning.

In this study, hot shear spinning experiments were conducted to investigate the formability of AZ31B alloy. Its microstructure and mechanical properties were studied at various temperatures, spindle speeds and feed ratios, and the effects of texture on the mechanical properties of hot shear spinning were analysed.

2 Experimental

Commercial Mg–3.0Al–1.0Zn–0.5Mn (AZ31B, wt%) sheets with a thickness of 3 mm were used in this experiment. Their microstructure was examined by electron backscatter diffraction (EBSD) in the rolled direction (RD)–transverse direction (TD) plane. The inverse pole figure (IPF) maps were measured at a step size of 1.0 μm. The EBSD data were obtained with TSL OIM analysis software, and data with a confidence index greater than 0.1 were used for texture. The tensile specimens with a gage length of 15 mm were cut parallel to the RD and TD and stretched to failure on a Zwick/Roell mechanical testing machine. The tensile rate was 1.0 mm/min.

Figure 1 shows the microstructure and tensile properties of as-received rolled AZ31B sheets. The IPF map shows that the sheet covered small equiaxial grains with an average grain size of 8 μm. The (0001) pole figure of the initial sheets exhibited a typical basal texture, with the *c*-axis of

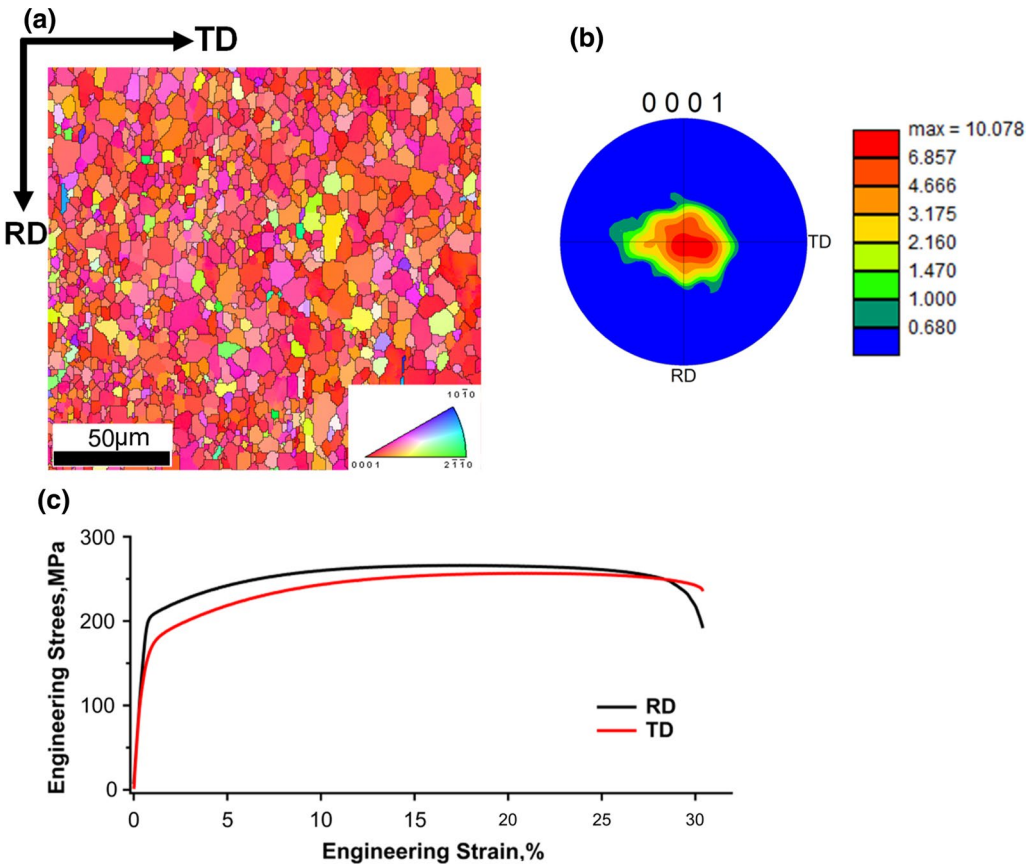

Fig. 1 **a** IPF map, **b** (0001) pole figure, **c** tensile stress–strain curve of initial AZ31B sheet

most grains parallel to the normal direction (ND). The peak intensity was tilted slightly away from the ND to the TD. Figure 1c demonstrates that the yield strength (YS), ultimate tensile stress (UTS) and elongation of the sheets in the RD were 203 MPa, 265 MPa and 30%, and those in the TD were 152 MPa, 256 MPa and 30.3%, respectively. The YS along the RD was 51 MPa higher than that in the TD. These findings demonstrate that the rolled sheet exhibited significant strength anisotropy due to its deflected texture.

The shear spinning experiments were carried out on a computer numerical control spinning machine with a single roller. Round sheets with diameter of 190 mm were cut from the as-received AZ31B sheets. Before the experiments, the round sheets were held for 10 min in an electric furnace at temperatures ranging from 373 to 673 K. The mandrel was preheated to the same temperature with electric heating pipes. In this process, the sheet and the mould were subjected to supplemental heat via flame heating. The scatter of temperature during the shear spinning was ± 10 K. The thickness reduction of shear spinning satisfied the sine law, $t = t_0 \sin a$, where t is the final thickness, t_0 is the initial thickness and a is the half-angle of the mandrel. In this study, t_0 was 3.0 mm, and a was 45°. Therefore, the final thickness was about 2.1 mm. After shear spinning, the spun sheets were immediately quenched in cold water to maintain their microstructure.

Figure 2 shows a schematic diagram of tensile samples and EBSD samples in the spun sheets. Two types of tensile samples with a gage length of 15 mm were cut from the spun sheets. The mid-section of the RD–TD plane of the spun sheets was prepared for EBSD to accurately capture the deformation texture. The test processes of mechanical properties and EBSD were as same as those for the initial rolled sheets.

3 Results

3.1 Effect of Annealing Process on Microstructure

The rolled sheets were preheated at various temperatures for 10 min in an electric furnace before the shear spinning experiments. Figure 3 shows IPF maps and (0001) pole figures of the annealed sheets at temperatures of 473 K, 573 K and 673 K. The grain size and grain orientation of the annealed sheets at 473 K were nearly the same as those of the initial sheets. It could be seen that the grains began to grow normally and that the average grain size increased to 12 μm after annealing at 573 K. However, some individual grains began to grow abnormally, and the largest grains exceeded 70 μm after annealing at 673 K. The pole figures show little change in the texture intensities relative to those of the rolled sheets after annealing at 473 K and 573 K. After annealing, the sheets still exhibited a typical basal texture, with the c-axis of most grains parallel to the ND. When annealed at 673 K, the basal texture became more dispersive, and the maximum basal texture intensity fell to 7.4. Abnormal grain growth is known to seriously reduce mechanical properties, especially elongation, which suggests that the shear spinning temperature of AZ31B sheets should be between 373 and 673 K.

3.2 Shear Spinnability of AZ31B Sheets

Shear spinnability is defined as the ability of a sheet to be formed into a desired shape according to a mould without fracturing [19]. Figure 4 shows the appearance of spun sheets conducted at temperatures from 373 to 673 K. Table 1 lists the process parameters and experimental results of hot shear spinning. When the shear spinning process was conducted at 373 K, cracks appeared during the initial stage and resulted in fracture at the bottom. When the deformation temperature exceeded 473 K, the sheets showed a good appearance, without cracks or wrinkling, during the shear spinning process. The sheets were successfully spun without

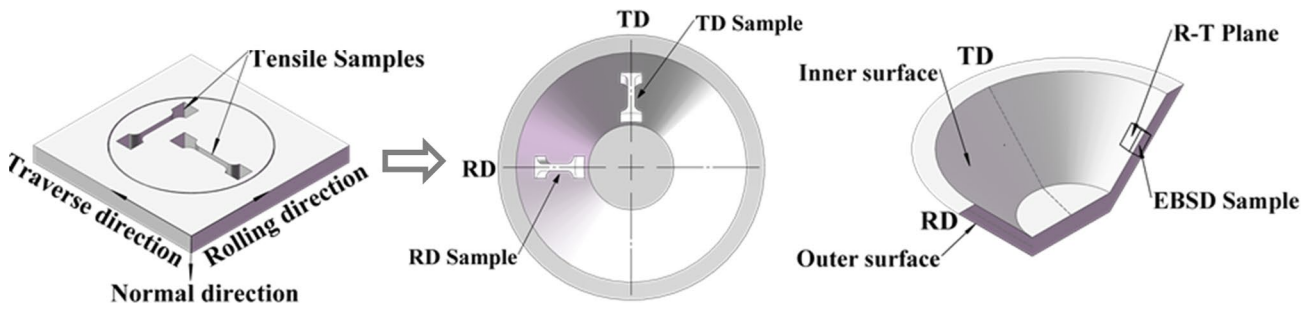

Fig. 2 Schematic diagram of tensile samples and EBSD samples in rolled and spun sheets

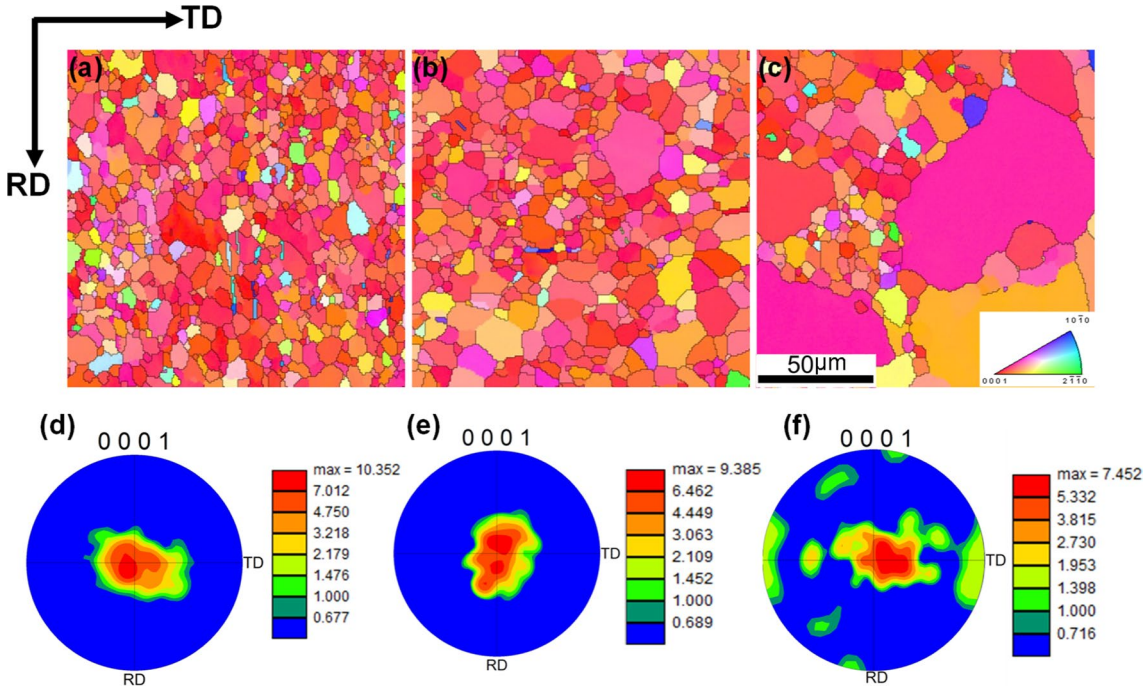

Fig. 3 IPF maps and (0001) pole figures of annealed AZ31B sheet for 10 min at **a**, **d** 473 K, **b**, **e** 573 K, **c**, **f** 673 K

Fig. 4 Oblique views of AZ31B sheets after hot shear spinning (373 K, 473 K, 573 K and 673 K)

Table 1 Process parameters used in this study

No.	Temperature (K)	Spindle speed (rev/min)	Feed ratio (mm/rev)	Result
1	373	300	0.1	Cracked
2	473	300	0.1	Fine
3	573	300	0.1	Fine
4	673	300	0.1	Fine
5	573	600	0.1	Fine
6	573	300	0.5	Fine

cracks over a temperature range from 473 to 673 K. Moreover, no cracks occurred after adjusting the spindle speed (300–600 rev/min) or the feed ratio (0.1–0.5 mm/rev) at 573 K. These results imply that temperature plays a more important role in the hot shear spinning of AZ31B sheets.

The ductility of Mg alloy is well known to improve dramatically above 473 K [20, 21]. Dislocation slip is activated to eliminate the pile-up of dislocation at elevated temperatures, reducing the stress concentration and preventing crack nucleation. Dynamic recrystallization improves the formability of Mg alloys by eliminating work hardening during hot deformation. Thus, the rolled AZ31B sheets exhibited good shear spinnability between 473 and 673 K due to the activation of more slip systems and dynamic recrystallization.

3.3 Effect of Temperature on Microstructure Development and Mechanical Property in Shear Spinning Process

Figure 5 shows IPF maps of the spun sheets at temperatures of 473 K, 573 K and 673 K. After shear spinning, the microstructure was composed of homogeneous and equiaxed grains. The average grain sizes were about 5, 8 and 15 μm after spinning at 473 K, 573 K and 673 K, respectively. Figure 6 displays the relationship between the average grain size and the annealing and spinning temperature. After shear spinning at 473 K, the average grain size was smaller than the grain sizes of the initial and annealed sheets. After shear spinning at 673 K, the average grain size was larger than the initial grain size and much smaller than the annealed grain size. It can be concluded that the grain was refined during the hot shear spinning process. Dynamic recrystallization is known to occur easily during hot plastic deformation in Mg alloys due to its low stacking fault energy, which is effective for grain refinement [22–26]. Twins are not observed after hot shear spinning, which indicates that dislocation glide

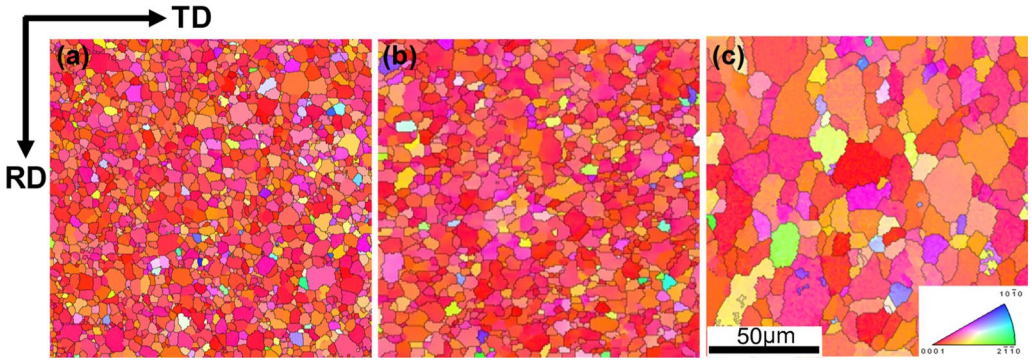

Fig. 5 IPF maps of spun sheets at various temperatures: **a** 473 K, **b** 573 K, **c** 673 K

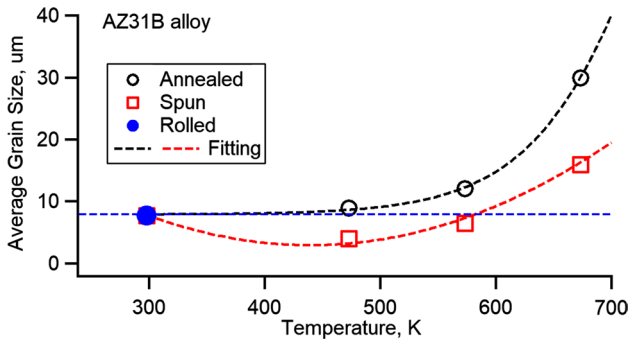

Fig. 6 Relationship of average grain size with annealed and spinning temperatures

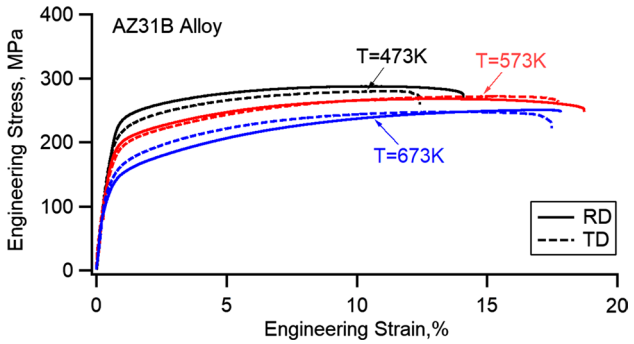

Fig. 7 Tensile stress–strain curves of spun sheets at various temperatures

and dynamic recrystallization are the dominant mechanisms during the hot shear spinning process.

Figure 7 shows the engineering stress–strain curves of the AZ31B sheet after shear spinning at temperatures of 473 K, 573 K and 673 K. Table 2 lists the related mechanical properties. After shear spinning at 473 K, the YS of the spun sheets along the RD and the TD was 221 MPa and 205 MPa, respectively. For spinning at 573 K, the YS decreased to

Table 2 Mechanical properties of spun sheets at various temperatures

No.	YS (RD/TD), MPa	UTS (RD/TD), MPa	Elongation (RD/TD), %
2	221/205	288/280	14.1/12.4
3	186/182	267/271	19.3/17.4
4	143/155	250/247	17.8/17.4

186 MPa and 182 MPa, and the UTS reached 267 MPa and 271 MPa along the RD and the TD, respectively. Moreover, the highest ductility in the RD and the TD (19.3% and 17.4%) was obtained for this condition. With an increase in temperature to 673 K, the YS along the RD and the TD reached 143 MPa and 155 MPa, respectively. The YS along the TD was much higher than that of the RD (by 12 MPa). Compared with the results for the initial sheet, the YS along the RD and the TD decreased by 60 MPa and 3 MPa. This illustrates that the tensile strength decreased as the deformation temperature increased. The discrepancy in the YS for the RD and TD samples decreased by 16 MPa, 4 MPa and 12 MPa after shear spinning at 473 K, 573 K and 673 K, respectively. The strength anisotropy of the spun sheet almost disappeared at 573 K. Therefore, a spun sheet can achieve both high strength and ductility when shear spinning is performed at a temperature below 573 K.

3.4 Effects of Spindle Speed and Feed Rate on Microstructure Development and Mechanical Property in Shear Spinning Process

Figure 8 shows the IPF maps of the spun sheets at 573 K with different spindle speeds (300–600 rev/min) and feed ratios (0.1–0.5 mm/rev). A few grains oriented in [10-10] and [2-1-10] appear in Fig. 8a. The average grain size of the spun sheets decreased slightly, from 7 to 5 μm, when the spindle speed increased from 300 to 600 rev/min.

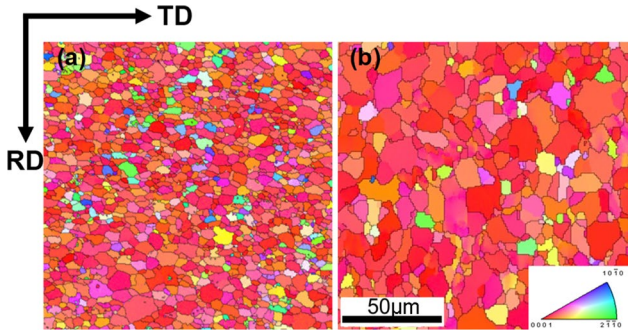

Fig. 8 IPF maps of sheets spun with different parameters: **a** 600 rev/min, 0.1 mm/rev, **b** 300 rev/min, 0.5 mm/rev

The average grain size reached 11 μm with a feed ratio of 0.5 mm/rev. Figure 9 shows the mechanical properties of the spun sheets corresponding to various spindle speeds and feed ratios. When the spindle speed increased from 300 to 600 rev/min, the YS and UTS along both the RD and TD of the spun sheets decreased to 160 MPa and 250 MPa, respectively. As the feed rate increased from 0.1 to 0.5 rev/mm, the YS of the spun sheets along the RD remained unchanged, but decreased by 15 MPa along the TD. This implies that the spindle speed and feed rate may not have significant effects on the microstructure and strength anisotropy (Table 3).

4 Discussion

4.1 Texture Development During Hot Shear Spinning Process

During the extrusion or rolling process, conventional Mg alloys usually develop a strong basal texture with the *c*-axis either perpendicular to the extrusion direction or parallel to the plane normal of the rolled sheet. However, few studies

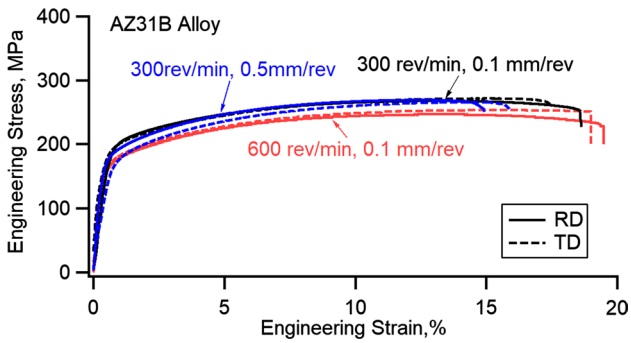

Fig. 9 Tensile engineering stress–strain curves of spun sheets with different spindle speeds and feed ratios

Table 3 Mechanical properties of spun sheets at different spindle speeds and feed ratios

No.	YS (RD/TD), MPa	UTS (RD/TD), MPa	Elongation (RD/TD), %
5	160/160	245/254	19.5/19.0
6	127/138	241/247	17.7/17.7

have discussed the texture development process during hot shear spinning.

Figure 10 shows (0001) pole figures of the spun sheets with various parameters. The spun sheets exhibited a typical basal texture, with the *c*-axis of most grains parallel to the ND. The maximum texture intensity was 12.7, 14.4 and 10.4 after spinning at 473 K, 573 K and 673 K, respectively. The effects of temperature on texture are achieved by activating slip systems and dynamic recrystallization. As non-basal slip is difficult to activate at low temperatures, the main slip mechanism is basal slip, so the *c*-axis of most grains is parallel to the direction of compressive stress, such as in the strong basal texture of a cold rolled sheet. However, as the temperature increases, the critical shear stress of non-basal slip decreases sharply, allowing non-basal slip to be activated to allow the *c*-axis of the grains to rotate into more directions, which can weaken the basal texture. Mabuchi et al. [27] reported that the basal texture disappeared after rolling at above 773 K because of the activation of non-basal slip and abnormal grain growth. The maximum texture intensity at 573 K is higher than that at 473 K after shear spinning, possibly as a result of shear stress. The AZ31B alloy presents poor ductility at 473 K, so that the effect of shear stress is more significant than that at 573 K, which leads to a weakened basal texture. This phenomenon is also observed in Mg alloys processed by rolling at different speeds.

Texture evolution is closely related to the stress state of the deformation zone. The texture of the spun sheets was much stronger than that of the rolled and annealed sheets. Figure 11 shows the complexity of the stress distribution at the deformation zone during shear spinning. The deformation zone of shear spinning can be divided into a main deformation zone (abc) and a bending zone (acde). The main deformation zone includes tensile stress σ_c and compressive stress σ_m generated by a mould. The main deformation zone is subjected to compressive stress σ_m, so that the (0001) basal planes are close to the plane of the sheet, leading to a stronger basal texture. The bending zone includes radial compressive stress σ_n and axial shear stress τ_0 generated by the roller. The shear stress τ_0 is perpendicular to the plane of the sheet, which causes the (0001) basal planes to rotate away from the plane of the sheet during hot spinning, thereby weakening the basal texture. As mentioned above, it

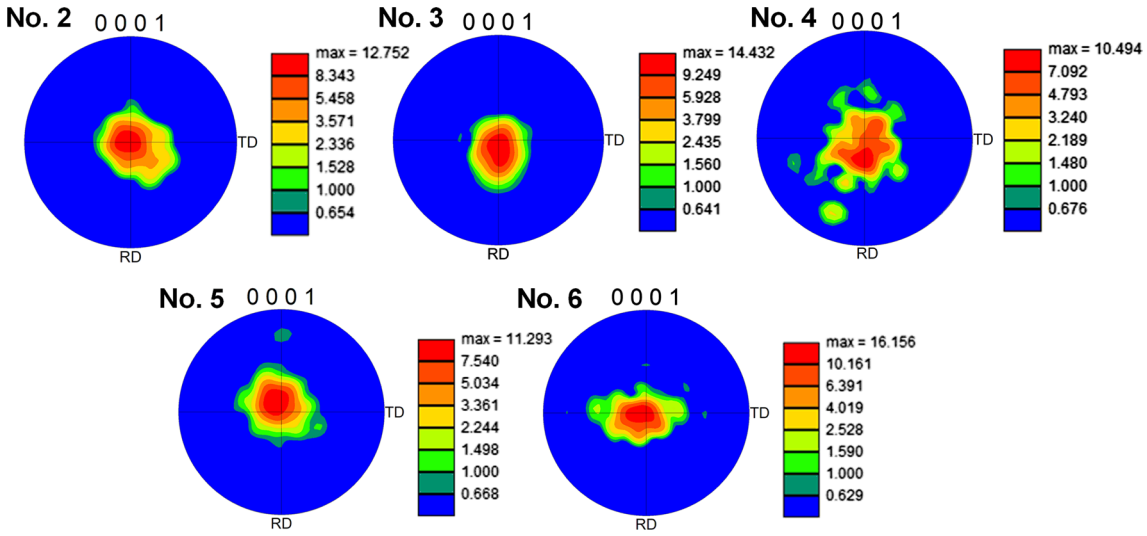

Fig. 10 (0001) pole figure of spun sheets: **a** 473 K, 300 rev/min, 0.1 mm/rev, **b** 573 K, 300 rev/min, 0.1 mm/rev, **c** 673 K, 300 rev/min, 0.1 mm/rev, **d** 573 K, 600 rev/min, 0.1 mm/rev, **e** 573 K, 300 rev/min, 0.5 mm/rev

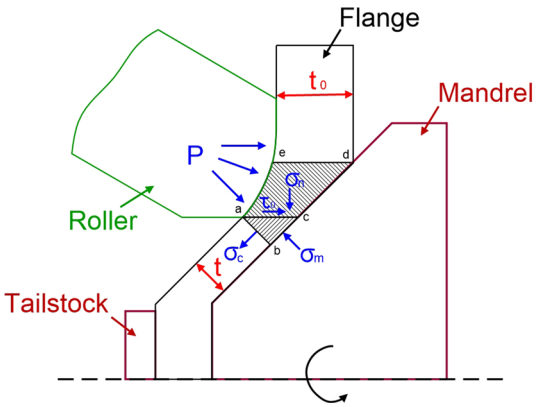

Fig. 11 Schematic of stress state in deformation area during shear spinning

can be inferred that the effects of compressive stress σ_m are dominant during hot shear spinning.

4.2 Effect of Texture on Mechanical Properties

A strong texture usually develops during the hot deformation of Mg alloys, which can significantly affect their mechanical properties [28–30]. Strength anisotropy is related to deformation texture of magnesium alloy [31]. In this study, the rolled sheets exhibited significant strength anisotropy with a greater YS in the RD samples. This shows that the rolled sheets exhibited a typical basal texture, with the *c*-axis of most grains parallel to the ND. The basal poles showed a greater angular spread towards the TD than the RD, indicating that the grains tend to oriented with their basal planes inclined more towards the TD than the RD. The sheets exhibited larger Schmid factors of basal slip under the loading axis along the TD than those loading along the RD. Thus, the soft basal slip mode could accommodate a more significant fraction of the strain under the loading axis along the TD and non-basal slip with higher critical shear stress under the loading axis along the RD. This made the RD samples stronger [5, 31]. After shear spinning, the strength anisotropy weakened. It nearly disappeared when the temperature reached 573 K and 673 K. The angular spread in basal pole figures along the TD was significantly weakened, indicating that Schmid factors for basal slip are identical under loading along both the TD and the RD. Therefore, the strength anisotropy of spun sheets is significantly weakened after shear spinning.

It is worth noting that the grain size decreased as the spindle speed increased. The average grain size of the spun sheets decreased slightly, from 7 to 5 μm, as the spindle speed ranged from 300 to 600 rev/min. However, the YS did not increase correspondingly. The YS decreased slightly, from 186 to 127 MPa, with the spindle speed ranging from 300 to 600 rev/min. Figure 12 shows the Schmid factor distributions of basal slip and prismatic slip when the loading direction was along the RD at different spindle speeds and a feed ratio of 0.1 mm/rev. Table 4 presents the statistical distribution of Schmid factors of the RD samples. When the Schmid factor exceeded 0.25, the fraction of the basal slip was higher with a spindle speed of 600 rev/min than with a spindle speed of 300 rev/min. When the Schmid factor exceeded 0.40, the fraction of prismatic slip was lower with a spindle speed of 600 rev/min than with a spindle speed of 300 rev/min. It can be inferred that the basal slip of a spun

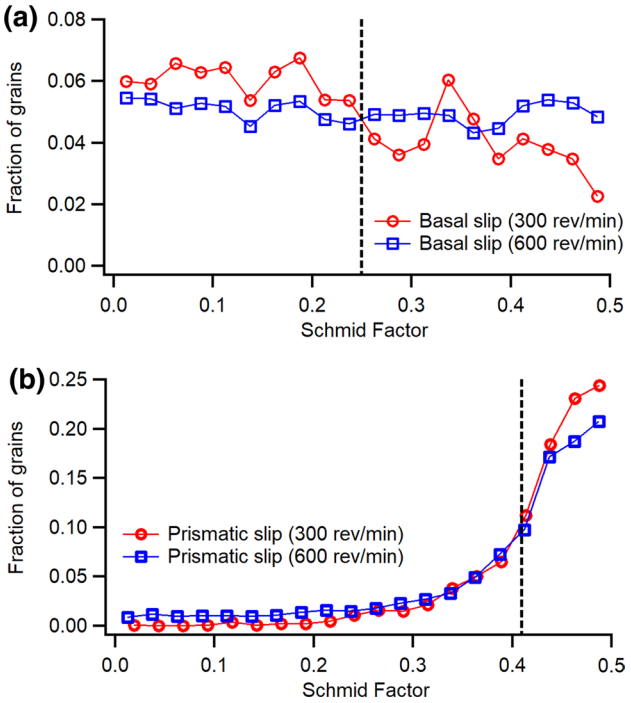

Fig. 12 Distributions of Schmid factors of RD samples with different spindle speeds

Table 4 Statistical distribution of Schmid factors of RD samples with different spindle speeds

No.	Fraction of basal slip		Fraction of prismatic slip	
	< 0.25	> 0.25	< 0.40	> 0.40
3	0.60	0.40	0.23	0.77
5	0.79	0.21	0.11	0.89

sheet is easy to activate, which compensates for the effects of fine grain strengthening and lowers the YS.

5 Conclusions

The effects of temperature, spindle speed and feed ratio on the microstructure, texture development and mechanical properties of AZ31B magnesium alloy sheets in the hot shear spinning process were studied. The major conclusions were as follows:

1. The AZ31B sheets had good spinnability by hot shear spinning when suitable process parameters were adopted: a temperature between 473 and 673 K, a spindle speed between 300 and 600 rev/min and a feed ratio range of 0.1–0.5 mm/rev.
2. Temperature had a great influence on grain size and texture due to dynamic recrystallization. Each of the spun sheets presented a strong basal texture, with the *c*-axis of most grains parallel to the ND.
3. When the shear spinning was carried out at 473 K, a spindle speed of 300 rev/min and a feed ratio of 0.1 mm/rev, high tensile properties were obtained: the YS, UTS and elongation reached 202 MPa, 280 MPa and 12.4% loading along the RD and 228 MPa, 284 MPa and 11.4% loading along the TD, respectively. The improvement of mechanical properties and weak strength anisotropy may be attributed to the refinement of the grain and the strengthening of basal texture.

Acknowledgements This work was supported by the National Natural Science Foundation of China (Nos. 51601112, 51701117) and the Shanghai Rising-Star Program (No. 17QB1403000).

References

[1] O. Music, J.M. Allwood, K. Kawai, J. Mater. Process. Technol. **210**, 3 (2010)
[2] M. Zhan, X. Wang, H. Long, Mater. Des. **108**, 207 (2016)
[3] S. You, Y. Huang, K.U. Kainer, N. Hort, J. Magnes. Alloys **5**, 239 (2017)
[4] X.J. Wang, D.K. Xu, R.Z. Wu, X.B. Chen, Q.M. Peng, L. Jin, Y.C. Xin, Z.Q. Zhang, Y. Liu, X.H. Chen, G. Chen, K.K. Deng, H.Y. Wang, J. Mater. Sci. Technol. **34**, 245 (2018)
[5] S.R. Agnew, Ö. Duygulu, Int. J. Plast. **21**, 1161 (2005)
[6] S.R. Agnew, O. Duygulu, Mater. Sci. Forum **419–422**, 177 (2003)
[7] T. Tu, X. Chen, J. Chen, C. Zhao, F. Pan, Acta Metall. Sin. (Engl. Lett.) **32**, 23 (2019)
[8] K. Sheng, L. Lu, Y. Xiang, M. Ma, Z. Wang, Acta Metall. Sin. (Engl. Lett.) **32**, 235 (2019)
[9] W. Jia, L. Ma, Q. Le, C. Zhi, P. Li, J. Alloys Compd. **783**, 863 (2019)
[10] H. Watanabe, H. Tsutsui, T. Mukai, M. Kohzu, S. Tanabe, K. Higashi, Int. J. Plast. **17**, 387 (2001)
[11] R. Panicker, A.H. Chokshi, R.K. Mishra, R. Verma, P.E. Krajewski, Acta Mater. **57**, 3683 (2009)
[12] L.C. Chan, X.Z. Lu, Int. J. Adv. Manuf. Technol. **71**, 253 (2014)
[13] S.S.A. Shah, M.G. Jiang, D. Wu, U. Wasi, R.S. Chen, Acta Metall. Sin. (Engl. Lett.) **31**, 923 (2018)
[14] W. Jia, F. Ning, Y. Ding, Q. Le, Y. Tang, J. Cui, Mater. Sci. Eng. A **720**, 11 (2018)
[15] Z. Cao, F. Wang, Q. Wan, Z. Zhang, L. Jin, J. Dong, Mater. Des. **67**, 64 (2015)
[16] Y. Zhang, F. Wang, J. Dong, L. Jin, C. Liu, W. Ding, J. Mater. Sci. Technol. **34**, 1091 (2018)
[17] L. Li, Z. Cai, H. Xu, M. Wang, J. Yu, Int. J. Adv. Manuf. Technol. **75**, 897 (2014)
[18] L. RadoviĆ, M. NikaČEviĆ, B. JordoviĆ, Trans. Nonferrous Met. Soc. China **22**, 991 (2012)
[19] C.C. Wong, T.A. Dean, J. Lin, Int. J. Mach. Tools Manuf. **43**, 1419 (2003)
[20] D.L. Atwell, M.R. Barnett, W.B. Hutchinson, Mater. Sci. Eng. A **549**, 1 (2012)
[21] S.R. Agnew, J.A. Horton, T.M. Lillo, D.W. Brown, Scr. Mater. **50**, 377 (2004)

[22] T. Al-Samman, G. Gottstein, Mater. Sci. Eng. A **490**, 411 (2008)
[23] J. Del Valle, F. Carreño, O.A. Ruano, Acta Mater. **54**, 4247 (2006)
[24] A. Galiyev, R. Kaibyshev, G. Gottstein, Acta Mater. **49**, 1199 (2001)
[25] C.D. Barrett, A. Imandoust, A.L. Oppedal, K. Inal, M.A. Tschopp, H. El Kadiri, Acta Mater. **128**, 270 (2017)
[26] Z. Cai, F. Chen, F. Ma, J. Guo, J. Alloys Compd. **670**, 55 (2016)
[27] M. Mabuchi, Y. Chino, H. Iwasaki, T. Aizawa, K. Higashi, Mater. Trans. **42**, 1182 (2001)
[28] H.Y. Chao, Y. Yang, X. Wang, E.D. Wang, Mater. Sci. Eng. A **528**, 3428 (2011)
[29] W.J. Kim, H.W. Lee, S.J. Yoo, Y.B. Park, Mater. Sci. Eng. A **528**, 874 (2011)
[30] S. Seipp, M.F.X. Wagner, K. Hockauf, I. Schneider, L.W. Meyer, M. Hockauf, Int. J. Plast. **35**, 155 (2012)
[31] S. Liang, H. Sun, Z. Liu, E. Wang, J. Alloys Compd. **472**, 127 (2009)